A MICROMECHANICS APPROACH TO PREDICT BURST PRESSURE IN CRACKED PIPELINES

Fernando Dotta
Fracture Mechanics and Structural Integrity Group – NVFRAC
Dept. of Naval Architecture and Ocean Engineering,
University of São Paulo
São Paulo, SP 05508-900, Brazil
Email: fernando.dotta@poli.usp.br

Claudio Ruggieri
Fracture Mechanics and Structural Integrity Group – NVFRAC
Dept. of Naval Architecture and Ocean Engineering,
University of São Paulo
São Paulo, SP 05508−900, Brazil
Email: claudio.ruggieri@poli.usp.br

Abstract: Predictive methodologies aimed at quantifying the impact of defects (e.g., cracks, blunt corrosion, inclusions, weld flaws, etc.) in oil and gas pipelines play a key role in fitness-for-service analysis including, for example, repair decisions and life-extension programs of onshore and offshore facilities. Conventional procedures used to assess the integrity of piping systems generally employ simplified failure criteria based upon a plastic collapse failure mechanism incorporating the tensile properties of the pipe material. These methods establish acceptance criteria for defects based on limited experimental data for low strength structural steels which do not necessarily reflect the actual failure mechanism (e.g., stable crack growth of the macroscopic defect prior to pipe collapse) nor do they address specific requirements for the high grade steels currently used. This study extends a micromechanical approach based upon the computational cell methodology to model ductile crack extension of longitudinal crack-like defects in a high strength pipeline steel, API 5L X60. A central focus of the paper is the application of the cell methodology to predict experimentally measured burst pressures for pre-cracked pipe specimens with different crack sizes. Numerical computations are conducted on detailed finite element models for the pipe specimens to describe crack extension with increased pressure. The numerical simulations demonstrate the effectiveness of the cell approach to describe crack growth response and to predict the burst pressure for the tested pipes. The present methodology holds a significant promise as an engineering tool to simulate ductile crack growth and to predict the burst pressure of thin walled tubular structures containing crack-like defects.

Keywords: Fracture Mechanics, R Curves, Computational Cells, Burst Pressure, Pipelines

1.   Introduction

Predictive methodologies aimed at quantifying the impact of defects in oil and gas pipelines play a key role in safety assessment procedures (such as, for example, repair decisions and life-extension programs) of in-service facilities. For damaged (cracked) structures, the material failure (leakage or sudden rupture) is most often preceded by large amounts of slow, stable crack growth until a critical crack size is reached. Conventional failure assessment procedures applicable to piping systems containing defects (*e.g.*, cracks, blunt corrosion, inclusions, weld flaws, etc.) generally employ simplified failure criteria derived from a plastic collapse analysis of the remaining ligament ahead of the crack-like defect (ASME B31−G,1984; Miller, 1988). Major construction codes applicable to piping systems generally make allowance for the presence of material damage by establishing acceptance criteria for defects which are based on limited experimental data applicable to low strength structural steels. Moreover, current structural integrity assessment procedures assume failure criteria which do not necessarily reflect the actual failure mechanism nor do they address specific requirements for high grade pipe steels currently used. For this case, failure assessments may be overly conservative and lead to unnecessary repair or replacement of in-service pipelines.

Under sustained ductile tearing of a macroscopic crack, large increases in the load-carrying capacity for the defective structure, as characterized by J-Δa resistance curves (R-curves), are possible beyond the limits given by conventional elastic and elastic-plastic (stationary crack) analysis. Simplified methods for defect assessment which utilize the often significant increases in toughness of these materials during ductile crack growth were incorporated in the so-called *R6* (CEBG Report R/H/R6, 1976) and *API 579* (API RP−579, 2000) procedures. These methods rely on the direct application of R-curves measured using small, laboratory specimens to surface defects. However, laboratory testing of fracture specimens to measure resistance curves (J-Δa) consistently reveals a marked effect of absolute specimen size, geometry, relative crack size (a/W) and loading mode (tension *vs*. bending) on R-curves. For the same material, deep-notch bend, SE(B), and compact tension, C(T), specimens yield low R-curves while shallow-notch SE(B)s, single-edge notch tension, SE(T), and middle-crack tension, M(T), specimens yield larger toughness values at similar amounts of crack growth. These effects observed in R-curves arise from the strong interaction between microstructural features of the material which govern the actual separation process

and the loss of stress triaxiality in the crack front region due to large-scale yielding. Consequently, advanced methodologies for realistic fracture assessments must include advanced procedures to *transfer* fracture resistance data measured using small laboratory specimens to structural components in engineering applications.

Recent research efforts to develop transferability models for ductile fracture behavior in ferritic steels employ micromechanics models incorporating material softening due to void growth. In particular, the *computational cell methodology* proposed by Xia and Shih (1995) and extended in a 3-D context by Ruggieri et al. (1996) and Gullerud et al. (2000) provides a realistic modeling of ductile crack extension to predict microscopic void growth within a layer of cells defined over the crack plane. Numerical analyses of fracture specimens using the cell model have predicted the effects of geometry on *R*-curves and measured crack front profiles with surprising accuracy (Ruggieri et al.,1996).

This study extends a micromechanics approach based upon the *computational cell methodology* to model ductile crack extension of longitudinal crack-like defects in a high strength pipeline steel. Laboratory testing of an API 5L X60 steel at room temperature using standard, deep crack C(T) specimens provide the data needed to measure the crack growth resistance curve for the material. In the computational cell model, ductile crack extension occurs through void growth and coalescence (by cell extinction) within a thin layer of material ahead of crack tip. This layer consists of cubic cell elements where void growth and strain softening are modeled by a 3-D form of the Gurson-Tvergaard (GT) dilatant plasticity theory. A simple scheme to calibrate material-specific parameters for the cells is also described. A central focus of the paper is the application of the cell methodology to predict experimentally measured burst pressures for pre-cracked pipe specimens. The experimental program includes longitudinally precracked 20" (508 mm) O.D. pipe specimens with 15.8 mm thickness containing an internal crack with notch depth (*a*) and notch length (*2c*) of 7×140 mm. Numerical computations are conducted on detailed finite element models for the pipe specimens to describe crack extension with increased pressure. The numerical simulations demonstrate the effectiveness of the cell approach to describe crack growth response and to predict the burst pressure for the tested pipes. The present methodology holds significant promise as an engineering tool to simulate ductile crack growth and to predict the burst pressure of thin-walled tubular structures containing crack-like defects.

2. Micromechanics Modeling of Ductile Crack Growth

Ductile fracture in metals is a multistep mode of material failure incorporating the combination of various and simultaneous mechanisms at the microscale level (Garrison and Moody, 1987). Such mechanisms are conveniently divided as follows: a) nucleation of microvoids from fracture or separation of inclusions, b) subsequent growth of widely separated and larger microvoids, c) localization of plastic flow and d) final coalescence of microvoids. Unlike cleavage fracture, which is a mechanism driven almost entirely by the local tensile stresses, inclusion of the microregime of ductile fracture in crack growth analyses is central to relate the material tearing behavior with a macroscopic (engineering) fracture parameter in a continuum framework. Experimental observations and computational studies show that the plastic strains for nucleation are small thereby causing minimal damage in the material ahead of the crack tip. Such feature enables simplification of the four-step failure process described above by assuming the growth of microvoids as the critical event controlling ductile extension. Figure 1(a) pictures the schematic path of a growing crack in a ductile material. The material layer enveloping the growing crack, which must be thick enough to include at least a void or microcrack nuclei, identifies a process zone for the ductile fracture which conveniently gives the necessary length dimension for the model. Void growth and coalescence in the layer will cause the surface tractions that the process zone exerts on its surrounding drop to zero.

Recent analytical efforts building upon the GT model prompted the development of a numerical approach using *computational cells*; a term recently coined by Xia and Shih (1996), X&S. X&S advocate a computational model for ductile growth which defines a single layer of void-containing, cubical cells having linear dimension *D* along the crack plane on which Mode I growth evolves. The cells have initial (smeared) void volume fraction denoted by f_0. The layer thickness (*D*) introduces a strong length-scale over which damage occurs; elsewhere, the background material obeys the flow theory of plasticity without damage by void growth. Material outside the computational cells, the "background" material, follows a conventional J_2 flow theory of plasticity and remains undamaged by void growth in the cells. As a further simplification, the void nucleates from an inclusion of relative size f_0 immediately upon loading. Progressive void growth and subsequent macroscopic material softening in each cell are described with the Gurson-Tvergaard (GT) constitutive model for dilatant plasticity (Gurson, 1977; Tvergaard, 1990) given by

$$\left(\frac{\sigma_e}{\overline{\sigma}}\right)^2 + 2q_1 f \cosh\left(\frac{3q_2\sigma_m}{2\overline{\sigma}}\right) - \left(1 + q_3 f^2\right) = 0 \tag{1}$$

where σ_e denotes the effective Mises (macroscopic) stress, σ_m is the mean (macroscopic) stress, $\overline{\sigma}$ is the current flow stress of the cell matrix material and f defines the current void fraction. Under multiaxial stress states, $\sigma_e = (3S_{ij}S_{ij}/2)^{1/2}$ where S_{ij} denotes the deviatoric components of Cauchy stress. Factors q_1, q_2 and q_3 introduced by Tvergaard improve the model predictions for periodic arrays of cylindrical and spherical voids. In the present analyses, we use $q_1 = 1.429$, $q_2 = 0.879$ and $q_3 = q_1^2$. These q-values are obtained from the work of Faleskog and Shih (1998) which provides the micromechanics param-

eters q_1 and q_2 for a wide range of material flow properties (strain hardening properties and yield stress) for common pressure vessel and structural steels. These adopted values correspond to flow properties for the tested API X60 pipeline steel presented next.

The GT yield function in Eq. (1) does not model realistically the rapid loss of stress capacity for larger void fractions nearing coalescence levels, nor does the model create new traction free surfaces to represent physical crack extension. Cell elements adjacent to the evolving crack front grow increasingly distorted under loading, especially for the small cell sizes commonly used ($D = 50$-$200 \, \mu$m)In the present work, the evolution of stress within cells follows the original constitutive model of GT in Eq. (1) until $f = f_E$, where f_E typically has a value of $\approx 0.15 \sim 0.20$. The final stage of void linkup with the macroscopic crack front then occurs by reducing the remaining stresses to zero in a prescribed manner. Tvergaard (1990) refers to this process as the element extinction or vanish technique. The cell extinction process adopted in this work implements a linear-traction separation model introduced by Ruggieri et al. (996), R&D. When f in the cell incident on the current crack tip reaches a critical value, f_E, the computational procedures remove the cell thereby advancing the crack tip in discrete increments of the cell size.
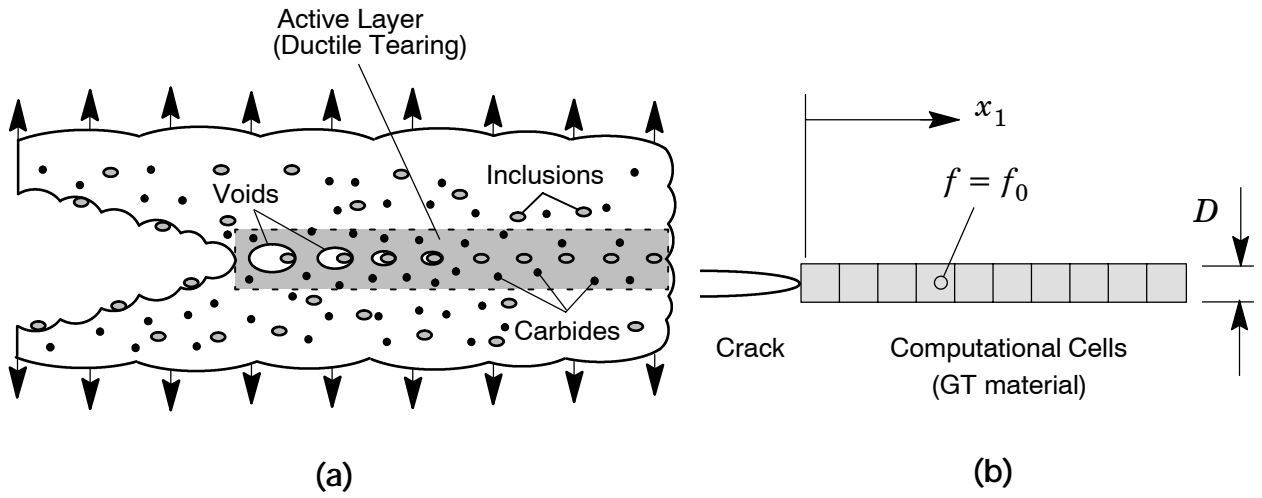
Figure 1 Modeling of ductile tearing using computational cells.

Figure 2 illustrates the cell extinction process coupled with such a linear-traction separation model. This scheme provides computational simplicity while, at the same time, retaining close contact with the physical mechanism of void coalescence just described. Figure 2(a) shows a deformed cell element with initial size normal to the crack (symmetry) plane of $D/2$; let $\overline{H}_0$ denote the average elongation of the cell normal to the crack plane as indicated in Fig. 2(a) when the porosity reaches the critical value, $f = f_E$. Forces, $\boldsymbol{P}_{vc}$, exerted on adjacent nodes by the remaining cell stresses are saved and the cell stiffness set to zero (vanished cells remain in the model but are marked inactive). During subsequent load increments, the now vanished cell continues to deform; let $\overline{H}$ denote the *current* average (deformed) elongation. The nodal forces $\boldsymbol{P}_{vc}$ are relaxed to zero in a linear fashion with subsequent increases of $\overline{H} - \overline{H}_0$, as shown in Fig. 2(b). At any point after $f = f_E$, the remaining fraction of nodal forces applied to the extinct cell is $\gamma \boldsymbol{P}_{vc}$, with γ given by

$$\gamma = 1.0 - \frac{\overline{H} - \overline{H}_0}{\beta \, (D/2)} \quad (0 \leq \gamma \leq 1) \tag{2}$$

where a typical value for the release factor, β, is 0.1.

This cell extinction process creates new traction free surfaces in a controlled manner and also eliminates numerical difficulties in the finite strain computations. Cell elements adjacent to the evolving crack front grow increasingly distorted under loading, especially for the small cell sizes commonly used ($D = 50$-$200 \, \mu$m). Compared to plane-strain models, the computations performed by Ruggieri et al. (1996) indicate this problem becomes far more acute in 3-D analyses. Non-uniform growth along the front (tunneling) causes local twisting of elements which would otherwise lead to inadmissible deformation gradients and termination of the analysis.

3. Experimental Program

To investigate the failure behavior of damaged pipelines, a series of full scale burst tests were performed on 20″ (508 mm) O.D., end-capped pipe specimens with 15.8 mm wall thickness and 3m length (Petrobrás, 2002a). These experimental tests are part of a pipeline integrity program conducted by the Brazilian State Oil Company (Petrobrás) and included both internal and external longitudinal notches with different sizes measured by notch depth and notch length, $a \times 2c$: 1) 3×60 mm, 2)
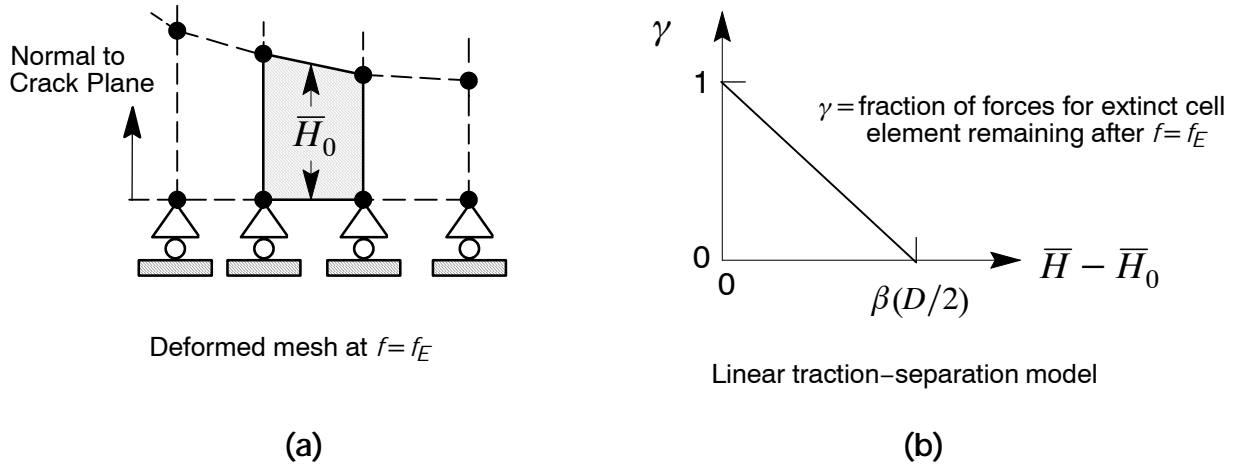
Figure 2 *Schematic illustration of the traction-separation model to release forces of extinct cell elements.*

7×140 mm and 3) 10×200 mm. The pipe specimens were notched along their length using an electrical discharge machine (EDM) to create the required notch shape. While the initial semi-elliptical defects were not subjected to a pressure cycle to propagate a fatigue crack from the original notch, the high accurate machining process allows considering them as initially blunted cracks. During the loading of the pipes, ductile crack extension was monitored by using an ultrasonic pulse technique to measure the crack growth (Petrobrás, 2002b).

The material is an API 5L Grade X60 pipeline steel with 483 MPa yield stress at room temperature (20 °C) and relatively low hardening properties ($\sigma_u/\sigma_{ys} \approx 1.2$). Tensile tests on round bar specimens (ASTM Standard Test Methods for Tension Testing of Metallic Materials - E8M) with 6 mm and 9 mm diameter extracted from the longitudinal orientation of the pipe provide the mechanical properties at room temperature (Petrobrás, 2002c). Figure 3 displays the engineering stress-strain data for this pipeline steel obtained using the round bar specimens (average of six tensile tests). Other mechanical properties for the material includes Young's modulus, $E = 210$ GPa and Poison's ratio, $\nu = 0.3$.

Laboratory testing of deep crack ($a/W = 0.5$) 0.5(T) side-grooved compact tension specimens with thickness $B = 13$ mm also provided the tearing resistance curves (J vs. Δa) at room temperature (20°C) to calibrate the cell parameters for the tested pipeline steel (Petrobrás, 2002d). Here a denotes the crack length and W the specimen width. The 0.5(T) C(T) specimens were tested at room temperature using a drop potential (DP) method to measure the crack growth resistance for the material. After fatigue pre-cracking, the specimens were side-grooved to a depth of 1 mm on each side to promote uniform crack growth over the thickness. Figure 4 presents the experimentally measured J vs. Δa curves. The fracture tests followed the procedures of ASTM Standard Test Method for Determining J-R Curves (E1152). Experimental J-values are determined using the measured load-load line displacement records.

4. Finite Element Procedures

Nonlinear finite element analyses are performed on plane-strain models for the side-grooved C(T) specimen and the longitudinally pre-cracked pipe specimen with an internal crack of 7×140 mm. The numerical computations for the crack growth analyses reported here are generated using the research code WARP3D (Koppenhoefer et al., 1994). Key features of the code employed in this work include: (1) the GT and Mises constitutive models implemented in a finite-strain setting, (2) cell extinction using a linear traction-separation model, (3) automatic load step sizing based on the rate of damage accumulation, and (4) evaluation of the J-integral using a domain integral procedure. The analyses utilize a piecewise-linear approximation of the measured engineering stress-strain curve for the API X60 steel shown in Fig. 3 with $E = 210$ GPa and $\nu = 0.3$. The matrix material of the computational cell elements and the void-free background material are assigned these properties.

Figure 5(a) shows the finite element model constructed for the plane-strain analyses of the 0.5-T C(T) specimen ($B = 13$ mm) with $a/W = 0.5$. Symmetry conditions permit modeling of only one-half of the specimen with appropriate constraints imposed on the remaining ligament. The half-symmetric model has one thickness layer of 1078 8-node, 3-D elements with plane-strain constraints imposed ($w = 0$) on each node. Displacement controlled loading applied at the pin hole indicated in Fig. 5(a) enables continuation of the analyses once the load decreases during crack growth. To simulate ductile crack extension, the finite element mesh contains a row of 130 computational cells along the remaining crack ligament ($W - a$) in a similar arrangement as shown in Fig. 1. The initially blunted crack tip accommodates the intense plastic deformation and initiation of stable crack growth in the early part of ductile tearing.
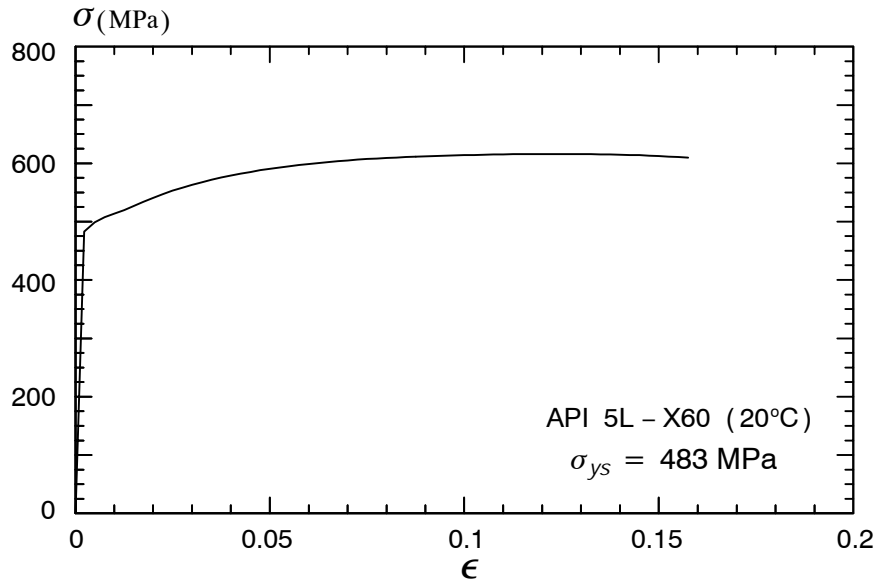
Figure 3 *Tensile response of tested API 5L Grade X60 Steel.*
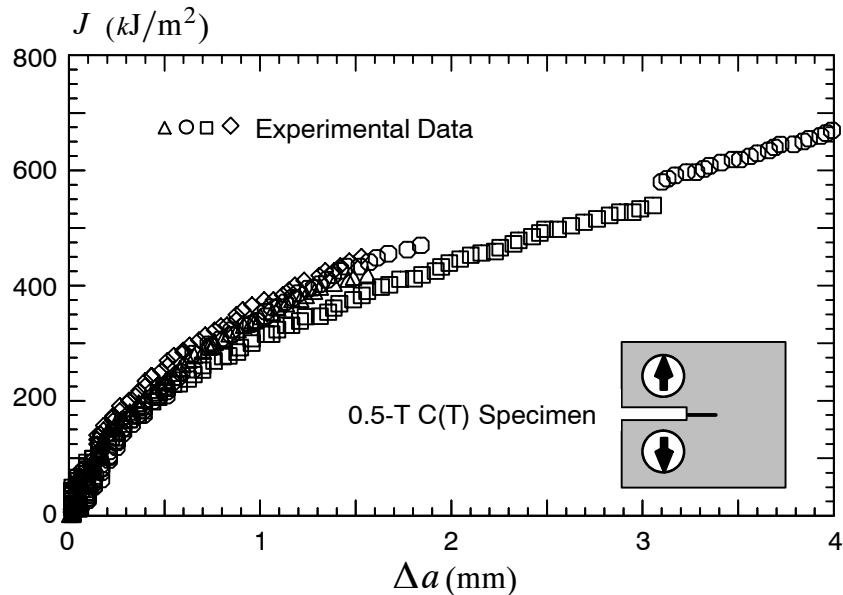
Figure 4 *Experimental R−curve for side-grooved 0.5-T C(T) specimen of API 5L-60 (20°C).*

Plane-strain finite element analyses are also conducted on the longitudinally cracked pipes with the 7×140 mm (internal) crack. Figure 5(b) shows the finite element model constructed for this pipe specimen. The half-symmetric model has one thickness layer of 1171 8-node, 3-D elements with plane-strain constraints ($w = 0$) imposed on each node. Here, the finite element mesh contains a row of 88 computational cells along the remaining crack ligament ($t - a$).

4.1. Calibration of Micromechanics Parameters

The parameters governing cell response, D and f_0, are calibrated using the deep notch C(T) specimen to establish agreement between predicted and measured R-curves (see Fig. 4). The calibrated values for these parameters are then applied in similar analyses to predict ductile extension in the pre-cracked pipe specimen. Guided by similar plane-strain analyses of X&S (1995) and experimental observations, the cell size is taken as $D/2 = 100 \, \mu$m for the tested material. This value of cell size is representative of the large inclusion spacing (thereby coupling to some extent the physical and computational model) while, at the same time, providing adequate resolution of the stress-strain fields in the near-tip material. With the length scale, D, fixed for the models, the calibration process then focuses on determining a suitable value for the initial volume
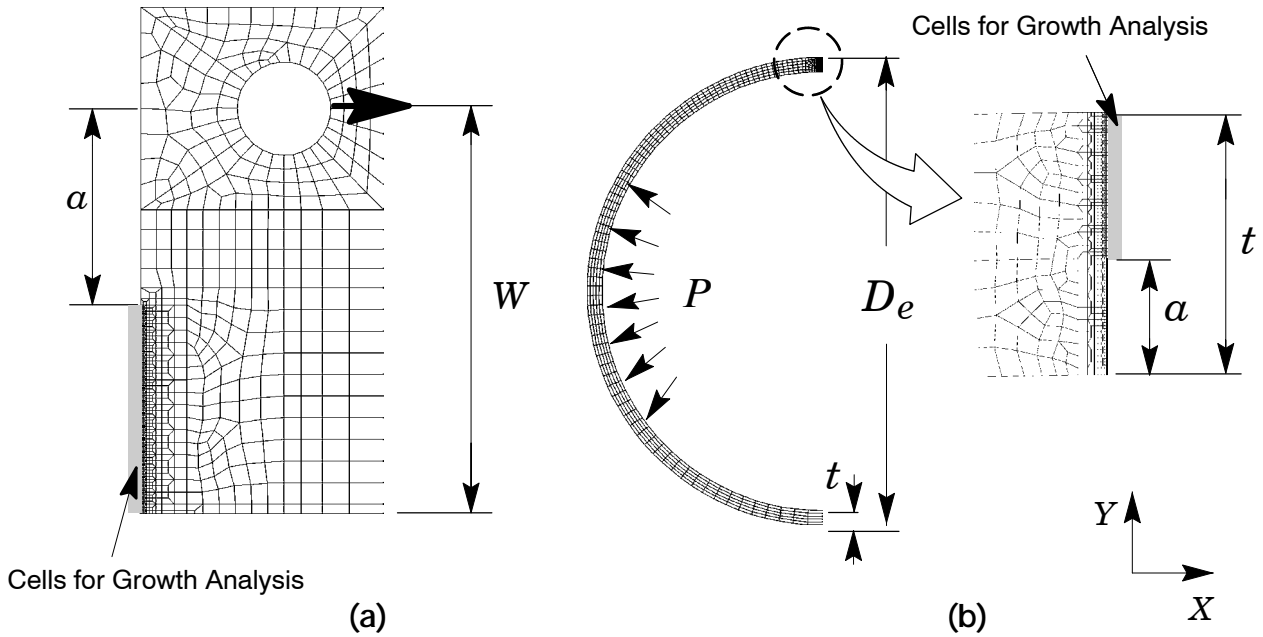
Figure 5 *Finite element models employed in the numerical analyses: a) plane-strain model of 0.5-T C(T) specimen with a/W = 0.5; b) plane-strain model of 20" O.D. pipe specimen with internal crack of 7 × 140 mm.*

fraction, f_0, that produces the best fit to the measured crack growth data for the deeply cracked specimens. Because each change in D requires construction of a new mesh, it is obviously much less effort to fix D early on and then calibrate f_0.

Figure 6 shows the measured and predicted J-Δa curves for the 0.5-T C(T) specimen. Predicted R-curves are shown for three values of the initial volume fraction, $f_0 = 0.01$, 0.008 and 0.0055. For $f_0 = 0.0055$, the predicted R-curve agrees well with the measured values for almost the entire crack extension range; for $\Delta a \geqslant 2$ mm the predicted curve lies a little above the measured data. In contrast, the use of $f_0 = 0.008$ and 0.01 produces a much lower resistance curve relative to the measured data. Consequently, the initial volume fraction $f_0 = 0.0055$ is thus taken as the calibrated (plane-strain) value for the API 5L-X60 steel used in the study.

5. Failure Assessment of Cracked Pipe

To verify the predictive capability of the micromechanics methodology adopted in the present work, this section describes application of the cell model incorporating the Gurson-Tvergaard damage criterion to predict the measured burst pressure for the longitudinally cracked pipe with the 7 × 140 mm internal crack. Very detailed nonlinear finite element analyses in plane strain setting enable simulation of ductile tearing under increased internal pressure for the pipe specimen. The numerical analyses adopt the cell parameters previously calibrated ($D = 200\,\mu$m and $f_0 = 0.0055$) as the material-specific parameters to predict the burst pressure for the pipe specimen.

Figure 7 shows the predicted and measured ductile crack extension with internal pressure, P. The solid symbols in the plots represent the measured crack growth for this pipe specimen. Under increased internal pressure, the amount of crack growth increases slowly up to $P \approx 23$ MPa. This pressure value marks the beginning of very rapid ductile tearing with little increase in the applied pressure. At $P25$ MPa, the load-carrying capacity of the remaining ligament cannot keep pace with the damage accumulation in the near-tip process zone (as characterized by the large number of damaged cell elements in the numerical model) so that an instability point is reached. Table 1 compares the measured and predicted burst pressure for the longitudinally cracked pipe with the 7 × 140 mm internal crack. The cell model prediction agrees fairly well with the experimental failure pressure for the analyzed pipe specimen.

Table 1 *Measured and predicted burst pressure for the 7 × 140 mm cracked pipe specimen (internal crack)*

	P (MPa) Experimental	P (MPa) Prediction
Plane-Strain Model	27.5	25
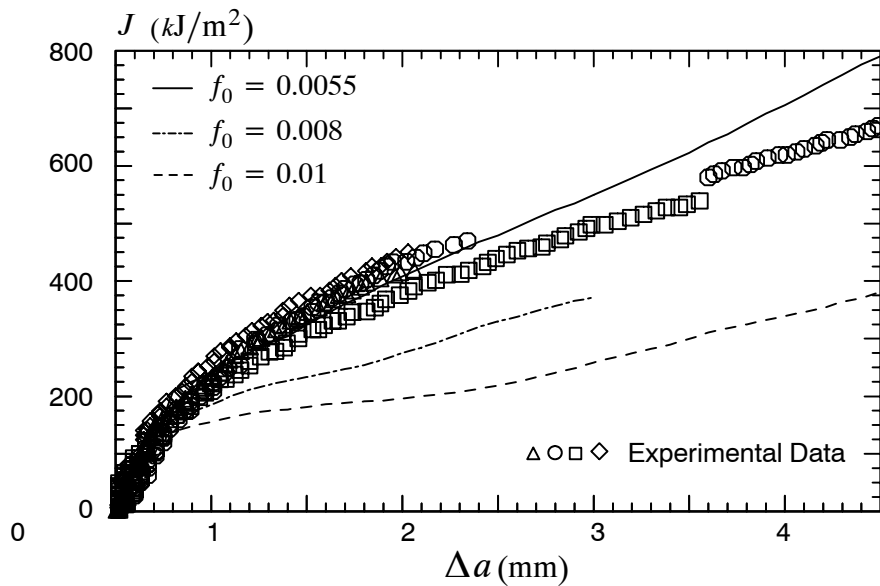
Figure 6 *Comparison of measured and predicted R-curve (plane-strain) for side-grooved 0.5-T C(T) specimen of API 5L-X60 at room temperature.*
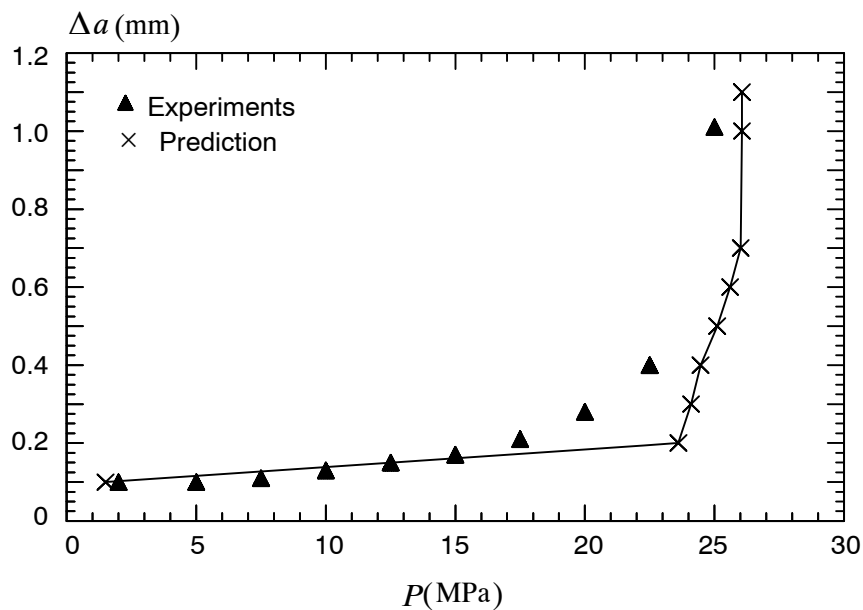
Figure 7 *Plane-strain predictions of ductile crack extension for the pipe specimen with 7 × 140 mm internal crack.*

6. Concluding Remarks

This study reports on an exploratory application of the computational cell model to analyze the ductile fracture behavior of a high strength, pipeline steel (API Grade 5L X60). Laboratory testing of a deep crack, compact tension specimen provides the tearing resistance characteristics of the material which is used to calibrate the material-specific parameter f_0. The model accurately reproduces the evolution of crack growth (Δa) with increasing loading, as measured by the J-integral, for this specimen. The cell model incorporating the calibrated cell parameters is then applied to predict the burst pressure of a thin-walled pipeline containing a longitudinal, internal shallow crack with $a \times 2c = 7 \times 140$ mm.

The plane-strain analyses reported here demonstrate the capability of the computational cell approach to simulate ductile crack growth and to correctly predict the burst pressure of the pre-cracked pipe specimen. Ongoing work with the com-

putational cell framework focuses on 3-D modeling of ductile tearing in cracked pipelines to resolve *R*-curve transferability issues and to incorporate more realistic failure and crack propagation criteria into the cell methodology.

7. Acknowledgements

8. References

American Petroleum Institute, "Recommended Practice for Fitness-for-Service", API RP-579, Washington, 2000.

Faleskog, J., and Shih, C.F., "Cell Model for Nonlinear Fracture Analysis - I: Micromechanics Calibration," *International Journal of Fracture*, Vol. 89, pp. 355-373, 1998.

Garrison, W. M, Jr. and Moody, N. R., "Ductile Fracture," *Journal of the Physics and Chemistry of Solids*, Vol. 48, pp. 1035-1074, 1987.

Gullerud, A. S., Gao, X., Dodds, R. H. and Haj-Ali, R., "Simulation of Ductile Crack Growth Using Computational Cells: Numerical Aspects," *Engineering Fracture Mechanics*, Vol. 66, pp. 65-92, 2000.

Gurson, A. L., "Continuum Theory of Ductile Rupture by Void Nucleation and Growth: Part I - Yield Criteria and Flow Rules for Porous Ductile Media," *Journal of Engineering Materials and Technology*, Vol. 99, pp. 2-15, 1977.

Harrinson, R. P., Loosemore, K. and Milne, I.., "Assessment of the Integrity of Structures Containing Defects," CEGB Report R/H/R6, Berkeley, U.K., 1976.

Koppenhoefer, K., Gullerud, A., Ruggieri, C., Dodds, R. and Healy, B., "WARP3D: Dynamic Nonlinear Analysis of Solids Using a Preconditioned Conjugate Gradient Software Architecture", *Structural Research Series (SRS) 596*, UILU-ENG-94-2017, University of Illinois at Urbana-Champaign, 1994.

Miller, A. G., "Review of Limit Loads of Structures Containing Defects," *International Journal of Pressure Vessels and Piping*, Vol. 32, pp. 197-327, 1988.

O'Dowd, N.P., and Shih, C.F., "Family of Crack–Tip Fields Characterized by a Triaxiality Parameter: Part I – Structure of Fields," *Journal of the Mechanics and Physics of Solids*, Vol. 39., No. 8, pp. 989–1015, 1991.

O'Dowd, N.P., and Shih, C.F., "Family of Crack–Tip Fields Characterized by a Triaxiality Parameter: Part II – Fracture Applications," *Journal of the Mechanics and Physics of Solids*, Vol. 40, pp. 939–963, 1992.

Petrobrás, "Burst Pressure Tests in 20" O.D. API Grade 5L X60 Pipelines," *Private Report*, 2002a (in Portuguese).

Petrobrás, "Tensile Tests in an API Grade 5L X60 Pipeline Steel," *Private Report*, 2002b (in Portuguese).

Petrobrás, "Ultrasonic Measurements in Burst Pressure Tests for a 20" O.D. API Grade 5L X60 Pipelines," *Private Report*, 2002c (in Portuguese).

Petrobrás, "*R*-Curve Measurements Using the Direct Potential Method for an API Grade 5L X60 Pipeline Steel," *Private Report*, 2002d (in Portuguese).

Ruggieri, C., Panontin, T. L. and Dodds, R. H., 'Numerical Modeling of Ductile Crack Growth in 3-D Using Computational Cells," *International Journal of Fracture*, Vol. 82, pp. 67-95, 1996.

The American Society of Mechanical Engineers, "Manual for Determining the Remaining Strength of Corroded Pipelines", ASME B31-G, New York, 1984.

Tvergaard, V., "Material Failure by Void Growth to Coalescence," *Advances in Applied Mechanics*, Vol. 27, pp. 83-151, 1990.

Xia, L. and Shih, C. F., "Ductile Crack Growth - I. A Numerical Study Using Computational Cells with Microstructurally-Based Length Scales," *Journal of the Mechanics and Physics of Solids*, Vol. 43, pp. 233-259, 1995.